

# Evaluation of elastic modulus and hardness of thin films by nanoindentation

Yeon-Gil Jung<sup>a)</sup> and Brian R. Lawn<sup>b)</sup>

*Materials Science and Engineering Laboratory, National Institute of Standards and Technology, Gaithersburg, Maryland 20899-8500*

Mariusz Martyniuk

*School of Electrical, Electronic and Computer Engineering, The University of Western Australia, Crawley, WA 6009, Australia*

Han Huang and Xiao Zhi Hu

*School of Mechanical Engineering, The University of Western Australia, Crawley, WA 6009, Australia*

(Received 7 May 2004; accepted 12 July 2004)

Simple equations are proposed for determining elastic modulus and hardness properties of thin films on substrates from nanoindentation experiments. An empirical formulation relates the modulus  $E$  and hardness  $H$  of the film/substrate bilayer to corresponding material properties of the constituent materials via a power-law relation. Geometrical dependence of  $E$  and  $H$  is wholly contained in the power-law exponents, expressed here as sigmoidal functions of indenter penetration relative to film thickness. The formulation may be inverted to enable deconvolution of film properties from data on the film/substrate bilayers. Berkovich nanoindentation data for dense oxide and nitride films on silicon substrates are used to validate the equations and to demonstrate the film property deconvolution. Additional data for less dense nitride films are used to illustrate the extent to which film properties may depend on the method of fabrication.

## I. INTRODUCTION

There is considerable interest in the use of instrumented nanoindentation as a means of characterizing mechanical properties of small-scale specimens, notably Young's modulus  $E$  and hardness  $H$ .<sup>1,2</sup> This is especially true of thin films on substrates. The practical importance of thin film systems makes it desirable to determine closed-form relations for  $E$  and  $H$  in terms of film thickness and properties of the constituent materials. Analytically, the problem is intractable because of the complicating influence of the film/substrate interface on the elastic and plastic stress fields. Some empirical relations have been proposed,<sup>3–11</sup> basically using variations on a rule of mixtures in combination with experimental or finite element modeling data. Any one of these empirical relations can generally be made to fit any given data set,

to a greater or lesser extent.<sup>3</sup> Deconvolution of film properties from measurements on the composite film/substrate bilayer is an ultimate goal.

In this study we propose a variant formulation for determining  $E$  and  $H$  of thin films from nanoindentation measurements. The approach follows that used by Hu<sup>12</sup> for spherical indenters on bilayers, here modified to accommodate the case of fixed-profile indenters, e.g., Berkovich or Vickers. A power-law function is used to relate  $E$  and  $H$  for the film/substrate composite to values for the constituent materials, with exponent dependent exclusively on indenter penetration relative to film thickness,  $h/d$ . Advantages of this approach are that the formulation is simple, the material and geometrical factors are separable, and the same formulation applies equally well where the stiffer/harder component comprises either the film or the substrate. Data for oxide and nitride films on a silicon substrate are used to evaluate coefficients in the  $E$  and  $H$  relations and to illustrate the utility of these relations as a means of deconvoluting the film properties.

## II. EXPERIMENT

Silicon with highly polished (100) surfaces (<1 nm surface finish) was chosen as our model substrate (University Wafer, South Boston, MA). For the bulk of the

<sup>a)</sup>On leave from Department of Ceramic Science and Engineering, Changwon National University, Sarim-dong 9, Changwon, Kyung-Nam, Korea.

<sup>b)</sup>Address all correspondence to this author.

e-mail: brian.lawn@nist.gov

DOI: 10.1557/JMR.2004.0380

studies, the silicon was coated with two kinds of films: (i) oxide, by thermal oxidation in moist oxygen atmosphere at 1100 °C; (ii) nitride, by low-pressure chemical vapor deposition (LPCVD) in  $\text{SiH}_2\text{Cl}_2/\text{NH}_3$  atmosphere at 830 °C. Films with thicknesses ranging from 50 nm to 1.5  $\mu\text{m}$  were deposited. X-ray diffraction was used to confirm that both kinds of film were amorphous. Scanning electron and atomic force microscopy indicated smooth film surfaces with roughness <10 nm and free of pores, indicating close to fully dense structures.

As a comparison case study, a different nitride film was fabricated by plasma-enhanced chemical vapor deposition (PECVD) in  $\text{SiH}_4/\text{NH}_3/\text{N}_2$  atmosphere at a low temperature of 100 °C. In this case, the film thickness was 500 nm. These films were again amorphous but rougher, with some porosity.

Nanoindentations (Nanoindenter XP, MTS Systems Corp., Oakridge, TN) were made on the film surfaces using a Berkovich indenter (tip radius <100 nm). Measurements were also made directly on some control silicon substrate surfaces (presumably with a natural oxide layer ~1 nm). Determinations of specimen  $E$  and  $H$  were made from load-displacement ( $P$ - $h$ ) curves,<sup>1</sup> over a range of indenter penetrations  $h = 70$  nm to 3  $\mu\text{m}$ . A Poisson's ratio  $\nu = 0.22$  (not a critical parameter) was used for all materials in the modulus evaluations. Atomic force microscopy (AFM) was used to confirm that the indents were well-formed over this penetration range.

### III. ANALYSIS

Consider the bilayer indentation system in Fig. 1, consisting of a homogeneous film of thickness  $d$  on a homogeneous substrate. A sharp, fixed-profile indenter is pressed onto the top surface at load  $P$ , with characteristic

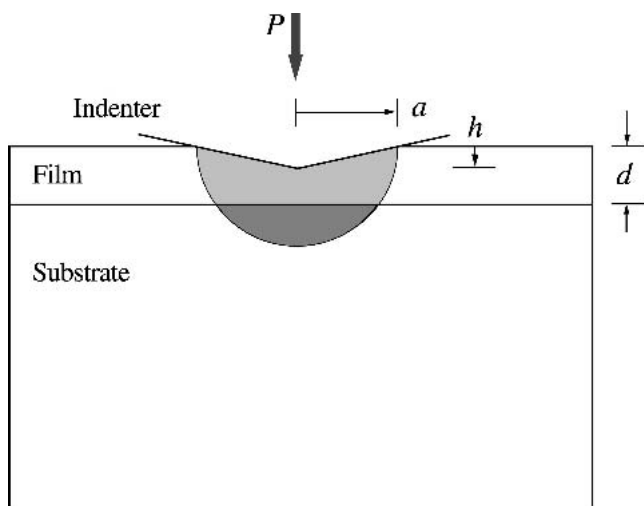


FIG. 1. Schematic illustration of fixed-profile nanoindentation on film/substrate system, indicating hemisphere of influence for deformation field.

contact radius  $a$  at full contact, or, equivalently, maximum penetration depth  $h$ . Assume that the volumes of influence of the elastic and plastic deformation fields are described by a hemisphere of radius  $a$ . Within the confines of this assumption, the principle of geometrical similarity<sup>13</sup> suggests that the deformation fields must have an invariant geometric form for a given ratio  $a/d$  or  $h/d$ . Then the elastic and plastic responses will change progressively from film-dominated at small  $a/d$  to substrate-dominated at large  $a/d$ , with the transition centered around  $a/d \approx 1$ ; i.e.,  $h/d \approx 1/7$  for Berkovich and Vickers indenters.<sup>2</sup>

Accordingly, we may expect modulus and hardness to be expressible as functions  $E(E_f, E_s, h/d)$  and  $H(H_f, H_s, h/d)$ , with subscripts f and s denoting film and substrate. Here we adapt a simple approach previously used by Hu<sup>12</sup> for spherical indentations, by writing modulus  $E$  and hardness  $H$  as power-law functions

$$E = E_s(E_f/E_s)^L, \quad (1a)$$

$$H = H_s(H_f/H_s)^M, \quad (1b)$$

where the exponent terms are dimensionless spatial functions  $L = L(h/d)$  and  $M = M(h/d)$ . This formulation conveniently separates material and geometry terms. Equation (1) must satisfy essential boundary conditions:  $h/d \rightarrow 0$ ,  $E = E_f$  and  $H = H_f$ ,  $L = 1$  and  $M = 1$  (small penetrations, film-dominated limit);  $h/d \rightarrow \infty$ ,  $E = E_s$  and  $H = H_s$ ,  $L = 0$  and  $M = 0$  (large penetrations, substrate-dominated limit). These boundary conditions are most simply and smoothly satisfied by sigmoidal functions

$$L = 1/[1 + A(h/d)^C], \quad (2a)$$

$$M = 1/[1 + B(h/d)^D], \quad (2b)$$

where  $A$ ,  $B$ ,  $C$ , and  $D$  are adjustable coefficients.

### IV. RESULTS

Plots of modulus  $E$  and hardness  $H$  as a function of indenter penetration  $h$ , for specified film thicknesses  $d$ , are shown in Fig. 2 for dense oxide and in Fig. 3 for dense (LPCVD) nitride films on silicon substrates. Each point is an average of about 10 nanoindentations. Standard deviation error bounds, omitted here to avoid excessive data overlap, are typically 10% of the means. Baseline  $E$  and  $H$  data for silicon substrates show no detectable variation with  $h$ , with means and standard errors  $E_s = 169.5 \pm 1.2$  GPa and  $H_s = 12.7 \pm 0.1$  GPa (32 data points, i.e., over 300 indentations). These data are omitted from Figs. 2 and 3 to avoid confusing overlap and are instead represented by horizontal dashed lines corresponding to mean values.  $E$  and  $H$  data sets for the film/substrate specimens all tend asymptotically to these

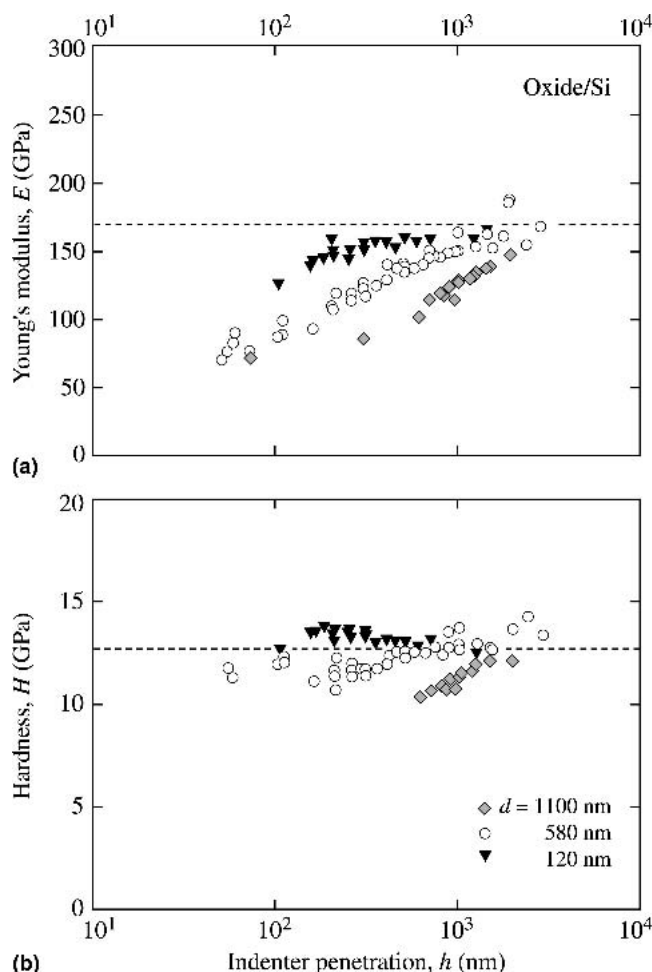


FIG. 2. Plots of (a) modulus  $E$  and (b) hardness  $H$  versus indenter penetration  $h$  for thermal oxide films on silicon, film thicknesses  $d$  indicated. Horizontal dashed line is mean for silicon.

dashed lines as  $h$  becomes large, as required. At the other end of the data range, as  $h$  becomes small,  $E$  and  $H$  tend downward or upward for oxide (Fig. 2) or nitride (Fig. 3) films, respectively. In each case the data sets shift to the right for films with larger  $d$ .

The modulus and hardness data for the oxide and nitride film systems in Figs. 2 and 3 are replotted in normalized form, modulus  $E(h/d)$  in Fig. 4 and hardness  $H(h/d)$  in Fig. 5. The data for each film system appear to reduce to universal curves, again asymptotically at large  $d$  to  $E_s = 169.5$  GPa and  $H_s = 12.7$  GPa for substrate silicon. Solid curves through the data are simultaneous regression best fits of Eqs. (1) and (2) to each data set, yielding common coefficients  $A = 3.76$ ,  $C = 1.38$ ,  $B = 1.47$ ,  $D = 1.71$ . These same best fits yield means and standard errors  $E_f = 72.5 \pm 1.5$  GPa and  $H_f = 11.5 \pm 0.2$  GPa for the oxide film (95 data points), and  $E_f = 266 \pm 4$  GPa and  $H_f = 35.0 \pm 0.3$  GPa for the nitride film (65 data points).

Finally, in Fig. 6 we compare modulus  $E(h/d)$  and hardness  $H(h/d)$  curves for the low-temperature PECVD

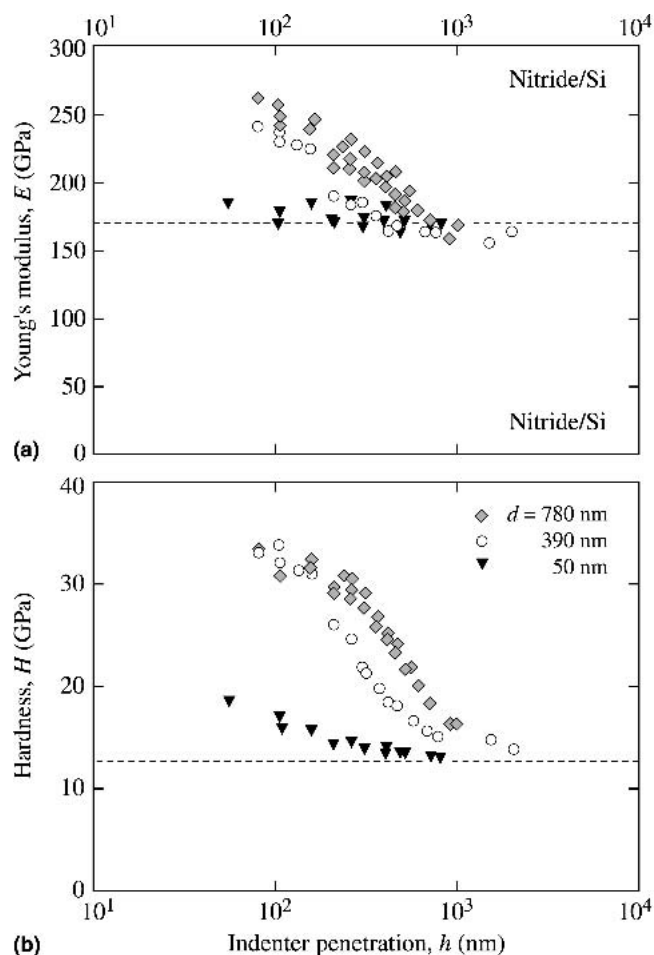


FIG. 3. Plots of (a) modulus  $E$  and (b) hardness  $H$  versus indenter penetration  $h$  for LPCVD nitride films on silicon, film thicknesses  $d$  indicated. Horizontal dashed line is mean for silicon.

nitride films with those for LPCVD nitride films from Figs. 4 and 5 (data for latter omitted). Curve fitting to the data in Fig. 6 yields relatively low values  $E_f = 119 \pm 3$  GPa and  $H_f = 11.5 \pm 0.3$  GPa for the PECVD nitride (means and standard errors, 36 data points), consistent with a higher defect content in this more porous film.

## V. DISCUSSION

We have proposed simple closed-form equations for predicting elastic modulus  $E$  and hardness  $H$  of film/substrate systems from constituent film and substrate properties. More importantly, these equations, once “calibrated,” make it possible to deconvolute film properties  $E_f$  and  $H_f$  from bilayer data. In principle, these evaluations may be made even without prior knowledge of substrate properties, but predeterminations of  $E_s$  and  $H_s$  considerably improve the accuracy. Clearly, the most accurate  $E_f$  and  $H_f$  determinations require data accumulation over as wide a range of  $h/d$  as possible, especially at small  $h/d$ . In the most favorable cases, for relatively

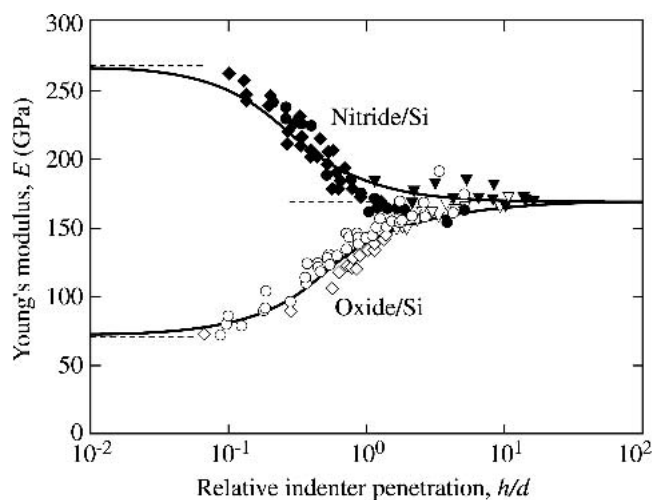


FIG. 4. Composite plots of oxide and nitride data, showing modulus  $E$  versus reduced indenter penetration (relative to film thickness),  $h/d$ . Data are shown from Figs. 2 and 3 (same symbols). Solid curves are best fits to Eqs. (1a) and (2a) for each material. Horizontal dashed lines are asymptotic limits for silicon (right) and film materials (left).

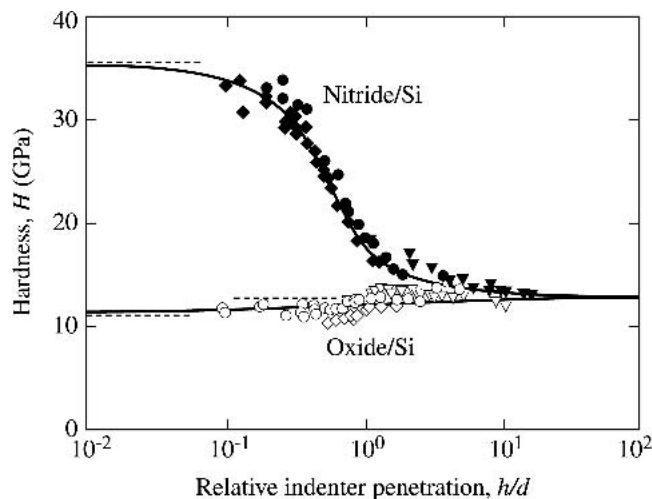


FIG. 5. Composite plots of oxide and nitride data, showing hardness  $H$  versus reduced indenter penetration,  $h/d$ . Data are shown from Figs. 2 and 3 (same symbols). Solid curves are best fits to Eqs. (1b) and (2b) for each material. Horizontal dashed lines are asymptotic limits for silicon (right) and film materials (left).

homogeneous films and prior knowledge of substrate properties,  $E_f$  and  $H_f$  may be estimated with an uncertainty of less than 10%. From the data trends in Figs. 4 and 5 it might be argued that reasonable first estimates could be obtained solely from data in the plateau region below  $h < 0.1d$ , without using any equations at all. However, a wider data range is always advisable, to confirm that the data have indeed saturated. In addition, there is a lower limit to the experimentally practical thickness  $h$ , without invoking indenter tip radius corrections. For our Berkovich indenter conditions this limit corresponds to  $h \approx 100$  nm, which precludes data in the plateau region

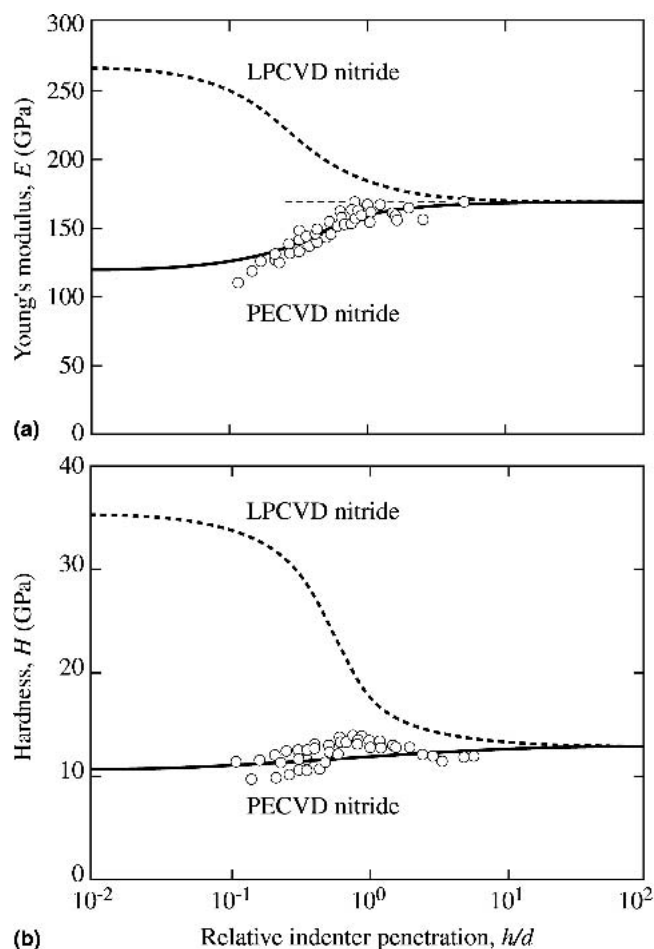


FIG. 6. Plots for low-temperature PECVD nitride data, (a) modulus  $E$  and (b) hardness  $H$ , for  $d = 500$  nm, plotted as function of relative penetration  $h/d$ . Solid curves through data are best fits to Eqs. (1) and (2). Dashed curves represent fits to LPCVD silicon nitride from Fig. 5.

for films of thickness  $d < 1$   $\mu\text{m}$ . In such cases, data extrapolation from the larger  $h/d$  region using Eqs. (1) and (2) is unavoidable.

As test of the validity of our formulation, we may compare present determinations of  $E_f$  and  $H_f$  from Figs. 4 and 5 with literature values for fully dense, homogeneous materials. In the case of the oxide film, we may expect the properties to be similar to those of bulk amorphous silica,  $\text{SiO}_2$ . Values cited in the literature for this material are in the vicinity of  $E = 70$  GPa and  $H = 10$  GPa, to within 10% or so. These values may be compared with  $E_f = 72.5$  GPa and  $H_f = 11.5$  GPa for our oxide film. It is more difficult to compare data for the nitride films with values for bulk silicon nitride—in the latter case, most literature data are reported on polycrystalline material, and are highly variable depending on microstructure (grain size, crystalline phase, additives, etc.).<sup>14</sup> Nevertheless, microindentation hardness on thick, dense CVD films using Vickers microindentations have been reported as high as 34 GPa,<sup>15</sup> which compares with

$H_f = 35$  GPa for our dense LPCVD nitride film. In the case of the low-temperature PECVD nitride in Fig. 6, we have no reliable basis for comparison, other than that the considerably lower hardness is expected because of the microstructural porosity.

Equations 1 and 2, even though empirical, constitute a simple and useful formulation for modulus and hardness determinations. It conveniently separates the material properties, expressed as a power-law relation [Eq. (1)], from the geometrical properties, contained solely within the sigmoidal exponent function [Eq. (2)]. These sigmoidal functions replace the Weibull functions used in the earlier Hu formulation,<sup>12</sup> with the advantage of smoother asymptotic solutions at  $h/d \rightarrow 0$ ; i.e., in the region critical to deconvolution of film properties. A feature of the formulation is that it applies equally well to hard/stiff films on soft/compliant substrates and vice versa. The relations have adjustable coefficients ( $A$ ,  $B$ ,  $C$ ,  $D$ ) that first need to be “calibrated.” We have done our calibration by fitting to experimental data for silicon substrates with well-defined oxide and nitride films. Similar calibrations could be effected by fitting to finite element data for specified material systems. The coefficients cannot be expected to be truly universal because different film/substrate material combinations will inevitably have different elastic/plastic zone geometries. In this context, the assumption of hemispherical deformation zones (Fig. 1) is oversimplistic. Special care may be warranted when comparing using the equations to predict responses of systems with films or substrates of different material types (e.g., ceramic, metal, polymer). Nevertheless, the formulation can be expected to be reliable in the evaluation of film properties for any given material class.

## ACKNOWLEDGMENTS

This work was sponsored by National Institute of Standards and Technology internal funds, by a grant to Yeon-Gil Jung from the Machine Tool Center at Changwon National University, Korea, and by grants from

the Australian Research Council and a Gledden Senior Fellowship.

## REFERENCES

1. W.C. Oliver and G.M. Pharr: An improved technique for determining hardness and elastic-modulus using load and displacement sensing indentation experiments. *J. Mater. Res.* **7**, 1564 (1992).
2. A.C. Fischer-Cripps: *Nanoindentation* (Springer-Verlag, New York, 2002).
3. P.M. Sargent: In *Micro Indentation Hardness Testing*, ASTM Special Technical Publication 899, edited by P.J. Blau and B.R. Lawn (ASTM, Philadelphia, PA, 1986), pp. 160-74.
4. P.J. Burnett and D.S. Rickerby: The mechanical properties of wear-resistant coatings. I. Modeling of hardness behavior. *Thin Solid Films* **148**, 41 (1987).
5. P.J. Burnett and D.S. Rickerby: The mechanical properties of wear-resistant coatings. II. Experimental studies and interpretation of hardness. *Thin Solid Films* **148**, 51 (1987).
6. A.K. Bhattacharya and W.D. Nix: Analysis of elastic and plastic deformation associated with indentation testing of thin films on substrates. *Int. J. Solids Struct.* **24**, 1287 (1988).
7. H. Gao, C-H. Chiu, and J. Lee: Elastic contact versus indentation modelling of multi-layered materials. *Int. J. Solids Struct.* **29**, 2471 (1992).
8. P-L. Larsson and I.R.M. Peterson: Evaluation of sharp indentation testing of thin films and ribbons on hard substrates. *J. Test. Eval.* **30**, 64 (2002).
9. T.Y. Tsui, C.A. Ross, and G.M. Pharr: A method for making substrate-independent hardness measurements of soft metallic films on hard substrates by nanoindentation. *J. Mater. Res.* **18**, 1383 (2003).
10. B. Bhushan: Nanomechanical characterization of solid surfaces and thin films. *Int. Mater. Rev.* **48**, 125 (2003).
11. A. Perriot and E. Barthel: Elastic contact to a coated half-space: Effective elastic modulus and real penetration. *J. Mater. Res.* **19**, 600 (2004).
12. X.Z. Hu and B.R. Lawn: A simple indentation stress-strain relation for contacts with spheres on bilayer structures. *Thin Solid Films* **322**, 225 (1998).
13. D. Tabor: *Hardness of Metals* (Clarendon, Oxford, 1951).
14. S.K. Lee, S. Wuttiaphan, and B.R. Lawn: Role of microstructure in hertzian contact damage in silicon nitride: I. Mechanical characterization. *J. Am. Ceram. Soc.* **80**, 2367 (1997).
15. I.J. McCollm: *Ceramic Hardness* (Plenum, New York, 1990), Table 6.9.